Journal of Radiation Research, 2012, 53, 672–685
doi: 10.1093/jrr/rrs019 Advance Access Publication 10 July 2012

Oxidative stress due to radiation in CD34$^+$ Hematopoietic progenitor cells: protection by IGF-1

Konstantina FLORATOU[1], Efstathia GIANNOPOULOU[2], Anna ANTONACOPOULOU[2], Marina KARAKANTZA[1], George ADONAKIS[3], Dimitrios KARDAMAKIS[4] and Panagiota MATSOUKA[5,*]

[1]Division of Hematology, Department of Medicine, University of Patras, Patras, Rio, 26504, Greece
[2]Clinical Oncology Laboratory, Division of Oncology, Department of Medicine, University of Patras, Patras, Rio, 26504, Greece
[3]Division of Obstetrics and Gynaecology, Department of Medicine, University of Patras, Patras, Rio, 26504, Greece
[4]Radiotherapy Division of Radiology, Department of Medicine, University of Patras, Patras, Rio, 26504, Greece
[5]Division of Hematology, University of Thessaly Medical School, University Hospital of Larissa, Larissa, 41110, Greece
*Corresponding author. Division of Hematology, University of Thessaly, Medical School, University Hospital of Larissa, Larissa, 41110, Greece. Tel/fax: 0030-241-3501625; Email: pmatsouka@med.uth.gr

(Received 20 December 2011; revised 9 March 2012; accepted 20 March 2012)

Radiation exerts direct as well as indirect effects on DNA through the generation of reactive oxygen species (ROS). Irradiated hematopoietic progenitor cells (HPCs) experience DNA strand breaks, favoring genetic instability, due to ROS generation. Our aim was to study the effect of a range of radiation doses in HPCs and the possible protective mechanisms activated by insulin-like growth factor-1 (IGF-1). ROS generation was evaluated, in the presence or absence of IGF-1 in liquid cultures of human HPCs-CD34$^+$ irradiated with 1-, 2- and 5-Gy X-rays, using a flow cytometry assay. Manganese superoxide dismutase (MnSOD) expression was studied by western blot analysis and visualized by an immunofluorescence assay. Apoptosis was estimated using the following assays: Annexin-V assay, DNA degradation assay, BCL-2/BAX mRNA and protein levels and caspase-9 protein immunofluorescence visualization. Viability and clonogenic potential were studied in irradiated HPCs. The generation of superoxide anion radicals at an early and a late time point was increased, while the hydrogen peroxide generation at a late time point was stable. IGF-1 presence further enhanced the radiation-induced increase of MnSOD at 24 h post irradiation. IGF-1 inhibited the mitochondria-mediated pathway of apoptosis by regulating the m-RNA and protein expression of BAX, BCL-2 and the BCL-2/BAX ratio and by decreasing caspase-9 protein expression. IGF-1 presence in culture media of irradiated cells restored the clonogenic capacity and the viability of HPCs as well. In conclusion, IGF-1 protects HPCs-CD34$^+$ from radiation effects, by eliminating the oxidative microenvironment through the enhancement of MnSOD activation and by regulating the mitochondria-mediated pathway of apoptosis.

Keywords: ionizing radiation; reactive oxygen species; MnSOD; IGF-1; hematopoietic progenitor cells

INTRODUCTION

In cancer patients undergoing therapeutic irradiation, hematopoietic progenitor cells (HPCs) are affected by direct bone marrow irradiation, or indirectly, by products from irradiated neighbouring tissues. Recent studies have shown that ionizing radiation on HPCs results in the generation of reactive oxygen species (ROS), influencing the oxidative status of the cells [1, 2]. ROS are products of normal cellular metabolism that act as second messengers in signal transduction pathways. They have the potential to modulate critical cellular components such as DNA, proteins and lipids, resulting in the activation of mechanisms that lead either to cell proliferation or to programmed cell death [3]. In several models of apoptosis due to various doses of radiation, increased generation of ROS has been described as an early event of apoptosis and as a cause of DNA strand breaks [4, 5]. Alternatively, radiation-induced oxidative

© The Author 2012. Published by Oxford University Press on behalf of The Japan Radiation Research Society and Japanese Society for Therapeutic Radiology and Oncology.
This is an Open Access article distributed under the terms of the Creative Commons Attribution Non-Commercial License (http://creativecommons.org/licenses/by-nc/3.0/), which permits unrestricted non-commercial use, distribution, and reproduction in any medium, provided the original work is properly cited.

stress results in mutations at target DNA loci, chromosomal rearrangements, epigenetic alterations and defective double strand breaks repair, contributing to the perpetuation of a genomic instability phenotype of the affected cells [6, 7].

Mutagenesis of DNA in critical repair genes and epigenetic alterations of DNA are responsible for the initiation of an instability phenotype [8, 9]. The progeny of irradiated cells display changes, such as aneuploidy, micronucleus formation, sister chromatid exchanges, gene mutations, amplifications and chromosomal destabilization, resulting in the generation of an aberrant clonal population of cells and promoting tumorigenesis [9].

Ionizing radiation has been shown to generate ROS in many cell types, through mitochondrial dysfunction [10, 11]. Endogenous generation of ROS and chronic exposure of cells to exogenously applied H_2O_2 have been linked with genomic instability and gene amplification [12]. Bone marrow cells in irradiated animals demonstrate alterations indicative of oxidative stress as well as mitochondrial damage [13]. Wang *et al.* have shown that total body irradiation caused residual bone marrow injury by induction of oxidative stress in murine hematopoietic cells [2].

Following irradiation, cells respond with an increase in the expression of cellular antioxidant defences, representing one of the most potent mechanisms of combating damage. Manganese superoxide dismutase (MnSOD), a scavenger of free radicals that exists predominantly in the mitochondrial environment, plays a central role in protecting cells against ROS injury during radiation exposure, catalysing the reaction of superoxide anion to hydrogen peroxide in the mitochondria of eukaryotic cells [14].

ROS generation has been also implicated in the activation of the mitochondrial pathway of apoptosis [15]. BCL-2 and BAX were among the first group of cell death regulatory genes identified as mediators of mitochondria-induced cell death. They have the potential to regulate the apoptotic cascade under a variety of stress conditions by modulating the mitochondrial transmembrane potential [16]. BCL-2 and BAX are both involved in the apoptotic cascade but it is important to note that their ratio constitutes the main factor for driving the cell to survival or death following an apoptotic stimulus [17, 18]. Caspase-9 represents an additional inducer of apoptosis, and is activated by cytochrome-c and Apaf-1 in the mitochondrial-mediated apoptotic cascade [19].

Numerous studies have shown the efficacy of growth factors in stimulating cell recovery after radiation-induced injury. G-CSF, GM-CSF, IL-3 and TPO are among the most efficient cytokines [20–22].

Insulin-like growth factor-1 (IGF-1) is a survival factor for a variety of cell systems [23]. HPCs and bone marrow stromal cells produce and secrete IGF-1, which, by binding to its receptor, regulates growth, differentiation and proliferation of hematopoietic cells with an autocrine or paracrine mechanism [22, 24]. IGF-1 induces pleiotropic responses in many cell types, acting as a survival factor and preventing the onset of apoptosis in stressed cells [25, 26]. The biological actions of IGF-1 are mediated by the IGF-1 receptor, a glycoprotein of the cell membrane. Binding of IGF-1 to the receptor promotes intrinsic tyrosine kinase activity leading to the activation of two main downstream signalling cascades, the mitogen-activated protein kinase (MAPK) and the phosphatidyl-inositol 3-kinase pathway [27, 28]. The phosphatidyl-inositol 3-kinase pathway activates via Akt signalling antiapoptotic (bcl-2, bcl-xl) or proapoptotic (Bax) proteins in mitochondria [29].

The aim of our study was to evaluate the biological effects of radiation and specifically the production of ROS and the initiation of programmed cell death on fresh isolated human $CD34^+$ HPCs, irradiated with a range of doses within the range of therapeutic doses commonly used in cancer patients. The hematopoietic cells characterized as $CD34^+$ are a cell population with functional heterogeneity and variability, involving stem cells and progenitor cells that retain both proliferation and differentiation potential (a proportion of these cells are in cell cycle or in G0 phase/dormant cells) [30].

Considering the known protective effects of IGF-1 on irradiated tissues [31], we investigated the effect of IGF-1 administration on irradiated HPCs-$CD34^+$ and the potential mechanisms triggered by the factor.

MATERIALS AND METHODS

Cell isolation and cultures conditions

Cord blood was obtained from the umbilical cord veins of healthy full-term human deliveries, after the informed consent of the mother. Umbilical cord blood cells was layered on Ficoll-Hypaque (Biochrom AG, Berlin, Germany, d = 1.077 g/ml). Mononuclear cells were collected by centrifugation on Ficoll-Hipaque and $CD34^+$ cells were isolated using CD34 positive magnetic beads (Miltenyi Biotec, Gladbach, Germany), according to the manufacturer's instructions. The purity of the isolated cells was evaluated by flow cytometry using a FITC-anti-CD34 antibody (Becton Dickinson, San Jose, CA) and the IgG1-FITC-antibody (Becton Dickinson) as a control. In all experiments the purity of HPCs-$CD34^+$ was close to 95%. The $CD34^+$ cell suspension was diluted to 25×10^3 cells/ml and cultured in iscove's modified dulbecco's medium (IMDM) (GIBCO, Paisley, UK) supplemented with 20% BIT (Stem cell Technologies-Vancouver, BC, Canada), 100 units/ml penicillin and 100 µg/ml streptomycin (Invitrogen, Molecular Probe, Leiden, The Netherlands). IGF-1 (R&D) diluted in phosphate buffered saline (PBS) was added to the cultures at a final concentration of 100 ng/ml, 15 min prior to irradiation.

Irradiation of cells

The suspensions of HPCs-CD34$^+$ were X-irradiated using a linear accelerator (Philips SL-75, Electa, Sussex, West England, UK) with 6-MV photons with doses of 1, 2 and 5 Gy. After the radiation the cells were incubated at 37°C with 5% CO_2. Non-irradiated HPCs-CD34$^+$ were used as control samples.

ROS generation

Generation of superoxide anion ($O2^-$) and hydrogen peroxide (H_2O_2) was measured at 30 min and at 24 h post-irradiation by flow cytometry using Hydriethidine dye (HE) and 2,7-dichlorofluorescein diacetate dye (2,7DCFH-DA), respectively, both dyes were from Molecular Probe. HE, a non-fluorescent lipophilic marker, is oxidized by $O2^-$ to the fluorescent hydrophilic product ethidium. In order to measure $O2^-$ generation, the cell suspensions were stained for 15 min at 37°C with 2.5 µl of a 63.5 mM HE solution in dimethyl sulfoxide (DMSO). The cells were washed once with PBS, resuspended in 200 µl of PBS and at least 5000 cells were analysed immediately by flow cytometry (FACS Calibur, Becton Dickinson) [10].

2,7DCFH-DA is a stable non-fluorescent, cell membrane-permeable compound dye, which, on penetrating the cell, is converted to DCFH by intracellular esterases, and then is trapped within the cell, remaining stable for a few hours. The desterilized product upon oxidation by H_2O_2 is converted to the highly fluorescent dichlorofluorescein (DCF) dye. Upon excitation at 488 nm DCF emits green fluorescence, proportional to the intracellular level of H_2O_2. The method is as follows: 2,7DCFH-DA (10 mM) was added to the cell suspension and incubated at 37°C for 15 min in the dark. Cells were washed once with PBS, resuspended in 200 µl of PBS, and at least 5000 cells were analyzed by flow cytometry (FACS Calibur, Becton Dickinson) [32].

The levels of ROS were monitored by the geometric means of fluorescence intensities of ethidium and DCF derived from the reduction of the HE and 2,7DCHF-DA fluorescent dyes, respectively [10].

Annexin-V and propidium iodide (PI) assay

Cell membrane changes that reflect the initiation of apoptosis were determined 6 h and 24 h after irradiation, by flow cytometry using an Annexin-V-FITC kit (Bender MedSystems, Vienna, Austria), according to the manufacturer's protocol. After the staining, at least 10 000 cells from each sample were analysed immediately by flow cytometry (EPICS-XL of Coulter, Miami, FL, USA).

DNA isolation and analysis

Six hours after irradiation, cells were harvested and washed twice with PBS. A standard procedure was followed for DNA isolation. Cells were resuspended in 20 µl of lysis buffer (50 mM Tris-HCl pH 8.0, 10 mM EDTA, 0.5% SDS and 0.5 mg/ml proteinase K) and incubated at 55°C for 60 min. Then, 5 µl of 1 mg/ml RNase A solution was added and the lysate was incubated at 55°C for another 60 min. The DNA samples were denaturated at 70°C for 5 min and analysed in a 1.5% agarose gel running for 4 h at 40 V. Ethidium bromide 0.5 µg/ml was added to the agarose solution for visualization of DNA bands. Pictures of the gel were captured under a source of UV light using a Kodak camera device.

Immunofluorescence assay

Twenty-four hours after irradiation, irradiated and non-irradiated HPCs incubated or not with IGF-1, were washed twice with PBS and were fixed on slides with a 4% paraformaldehyde in PBS buffered solution for 10 min at room temperature. They were rinsed 3×5 min with PBS, followed by a 1-h incubation in a 3% bovine serum albumin (BSA) solution supplemented with 10% free bovine serum (FBS) at 37°C. After incubation with blocking solution, cells were rinsed once with PBS for 5 min and treated overnight at 4°C with rabbit polyclonal antibodies (MnSOD 1:250 and caspase-9 1:250, Santa Cruz Biotechnology, CA, USA) diluted in blocking solution. Cells were rinsed 3×5 min with PBS and then an anti-rabbit antibody conjugated with Alexa Fluor 594 (1:500, Invitrogen, Molecular probe) diluted in blocking solution was added for 30 min at 37°C. Cells were rinsed 3×5min with PBS and mounted on glass slides. Nuclear staining was obtained using TOTO-3 IODIDE (Invitrogen, Molecular Probe). Fluorescence was visualized using a Leica microscope. We studied two specimens for each sample and four different fields per specimen. Each field included 12–15 cells. Two independent experiments were evaluated per each sample. We observed that the total cell population of studied cells was positive for MnSOD and caspase-9 expressions. Differences between the groups (irradiation with or without IGF-1) were depicted in the intensity of fluorescence.

Western blot analysis

Samples with 30 µg total amount of protein were diluted in 2X sample buffer and heated for 5 min at 95°C. Protein lysates were loaded in 10% SDS-PAGE gels, analysed and transferred to a nitrocellulose membrane (Schleicher and Schuell Bioscience, GmbH, Germany). For detection of MnSOD, BCL-2 and BAX, blocking was performed by incubation of the membranes in 5% (w/v) non-fat dry milk in Tris-buffered saline pH 7.4 containing 0.05% Tween 20 (TBS-T), for 1 h at room temperature and under continuous agitation. The membranes were then incubated with the appropriate monoclonal antibody (anti-MnSOD: Santa Cruz Biotechnology, dilution 1:1000, rabbit anti-Bax polyclonal: Chemicon, Millipore, Temecula, CA, USA, dilution 1:2000, and mouse Anti-Bcl-2, clone 100 monoclonal Upstate, Lake Placid, NY, USA, dilution 1 µg/ml) in 3%

(w/v) non-fat dry milk in TBS-T, for 2 h, at room temperature, under continuous agitation. After three washes in TBS-T, the membranes were further incubated with horseradish peroxidase-conjugated goat anti-rabbit IgG (MnSOD and BAX), and anti-mouse IgG (BCL-2), (Upstate, dilution 1:5000) in 3% (w/v) non-fat dry milk in TBS-T, for 1.5 h, at room temperature, under continuous agitation. Detection of the protein was performed by chelumínescence horseradish peroxidase substrate SuperSignal (Pierce, Rockford, IIL, USA), according to the manufacturer's instructions. As a control, the membranes were stripped and reprobed with a monoclonal antibody against actin. Quantitative analysis of protein expression was performed with ScnImage software.

RNA isolation and cDNA synthesis

Four hours after irradiation, irradiated and non-iraddiated HPCs-CD34$^+$ with or without IGF-1 addition were washed twice with PBS and total RNA was isolated using RNeasy mini kit (Qiagen, Valencia, California, USA) according to the manufacturer's instructions. The integrity of RNA was confirmed by visualization of ribosomal bands in EtBr-stained agarose gels. Total RNA from each sample was quantified using Ribogreen (Molecular Probes) and the MX3000p (Stratagene, La Jolla, CA, USA) according to the manufacturer's instructions. cDNA was synthesized from 10 ng of total RNA from each sample using random nonamers (ITE, Crete, Greece) and 50 U Stratascript reverse transcriptase (Stratagene). Human Reference RNA (Stratagene) was used as a calibrator sample to allow for adjustment for run-to-run variation. A non-enzyme control was also included [33].

Real time PCR

BCL-2 and BAX mRNA were quantified using Taqman chemistry and Brilliant quantitative PCR core reagents (Stratagene). Primers for BCL-2 and BAX genes were designed using Primer3 [34] and synthesized at the Institute of Technology (Crete, Greece).

All reactions were performed in MX3000p (Stratagene), in duplicate, and contained 5-carboxy-x-rhodamine as a passive reference dye and cDNA equivalent to 30 ng of RNA. A standard curve was always included for assay validation. In addition, a melting curve analysis was performed for the SYBR Green I assay. The relative abundance of mRNA of the gene of interest was deducted from the cycle number at which fluorescence increased above background level (Ct) at the exponential phase of the PCR reaction, after normalization to the Ct of the calibrator sample [33]. The ratio of BCL-2/BAX was calculated dividing mRNA levels of BCL-2 and BAX, respectively, derived from the same experiment.

MTT assay

The viability of non-irradiated and irradiated HPCs-CD34$^+$ cells, in the presence or absence of IGF-1, was determined with the 3-[4,5-dimethylthiazol-2-yl]-2,5-dimethyltetrazolium bromide assay (MTT), 48 h after irradiation [28]. Briefly, cells were seeded at a density of 25×10^3cells/well in 24-well tissue culture plates. Forty-eight hours after irradiation MTT (5 mg/ml in PBS) was added at a volume equal to 1/10 of the medium culture and the plates were incubated at 37°C for 2 h. The cells were harvested and washed with PBS pH 7.4, and 100 μl of acidified isopropanol (0.33 ml HCl in 100 ml isopropanol) was subsequently added to each well to dissolve the dark blue formazan crystals. The plates with the cell lysate were immediately read at a wavelength of 492 nm on a microplate reader (Tecan, Sunrise, Magellan 2, Grodig, Austria).

Clonogenic assay

Irradiated and non-irradiated HPCs-CD34$^+$cells, incubated or not with IGF-1 were washed twice with IMDM and plated in 35-cm cell culture dishes at a density of 1000 cells/dish, in complete media of 1% methylcellulose IMDM, 30% FBS supplemented with 1% BSA, 2 mM L-glutamine, 10^{-5} M 2-mercaptoethanol, and a cocktail of growth factors (50 ng/ml stem cell factor, 20 ng/ml granulocyte-macrophage colony stimulating factor, 20 ng/ml granulocyte colony-stimulating factor, 20 ng/ml rh-interleukin-3 and 3 U/ml rh-erythropoietin, all from Stem Cell Technologies). Cell colonies were counted in an inverted microscope (Olympus) 10–14 days after the plating. Aggregates of >20 cells were considered as colonies [35, 36].

Statistical analysis

Results are expressed as mean ± SE from at least three independent experiments and were analysed using the SPSS program using a one way-ANOVA test. A P value of <0.05 was considered as statistically significant. In cases where no statistical difference was observed, the P value is not mentioned in the figures.

RESULTS

Radiation-induced ROS generation in CD34$^+$ HPCs and the IGF-1 effect

Superoxide anion levels appeared to rise as early as 30 min after irradiation in a dose-dependent manner. This linear increase was reversed in the presence of IGF-1, restoring O_2^- generation to the levels of the innate production as observed in the control, non-irradiated samples (Fig. 1A). The levels of superoxide anion were 122.48 ± 6.14, 132.2 ± 1.90, 146.6 ± 0.90 and 150.8 ± 5.33 after 0, 1, 2 and 5 Gy respectively, and returned to 111.74 ± 6.81, 123.6 ± 3.52, 131.9 ± 3.80 and 124.8 ± 2.76 in the presence of IGF-1, giving statistical differences at 2 and 5 Gy (Fig 1A). Twenty-four hours post-irradiation, superoxide anion levels remained high but the increase observed was not dose-dependent as no statistical differences were noted among the irradiated and non-irradiated samples. A reduction of superoxide anion generation was noted under IGF-1

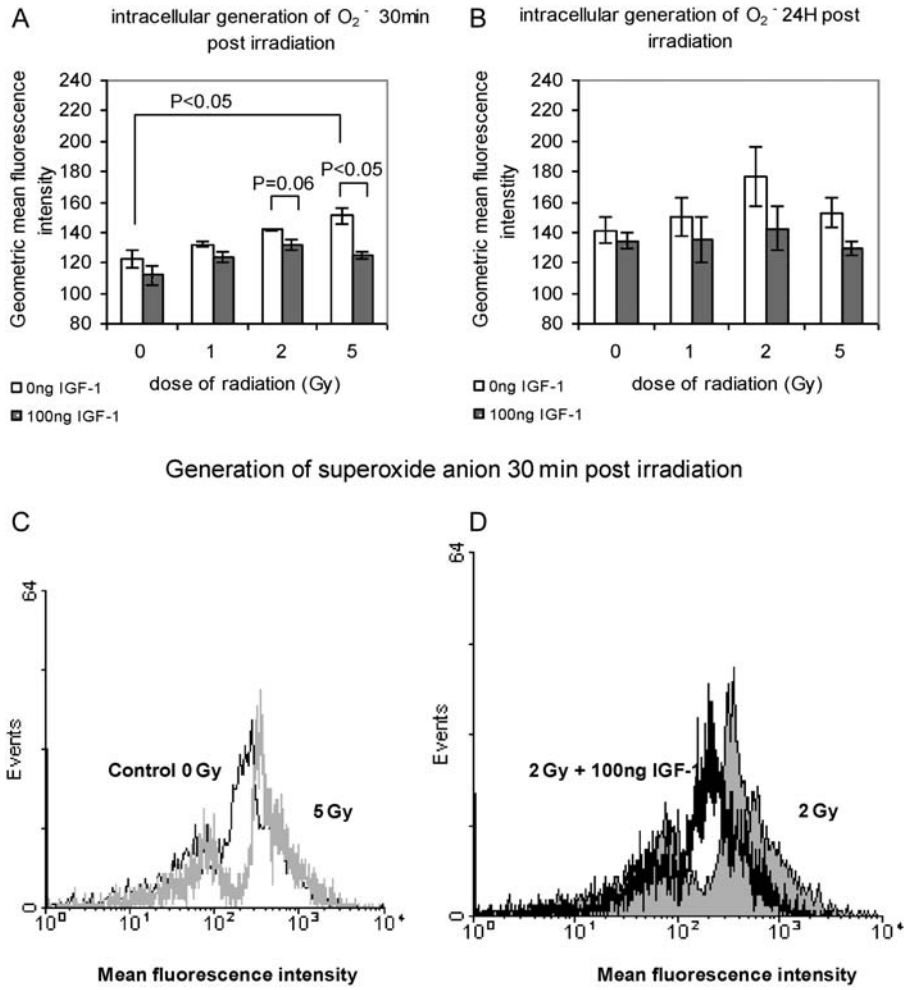

Fig. 1. Superoxide anion generation in irradiated HPCs-CD34$^+$ at 30 min (**A**) and at 24 h (**B**) post-irradiation with 1, 2 and 5 Gy; (**C**) representative flow cytometry histogram showing superoxide anion levels in non-irradiated and irradiated with 5 Gy HPCs-CD34$^+$ cells; (**D**) representative flow cytometry histogram showing superoxide anion levels in HPCs-CD34$^+$ cells irradiated with 2 Gy and the protective effect of IGF-1. The values represent the mean ± SE of at least three independent experiments. In (C) the increase of the superoxide anion levels is indicated by the shift of the histogram to the right, and in (D) the protective effect of the IGF-1 is indicated by the shift of the histogram to the left.

presence, 24 h post-irradiation (controls/0 Gy: 134 ± 5.48 vs 141 ± 8.7, 1 Gy: 135 ± 14.73 vs 150 ± 12.83, 2 Gy: 142 ± 14.69 vs 176 ± 19.49 and 5 Gy: 129 ± 4.63 vs 153 ± 9.86; Fig. 1B). A representative flow cytometry histogram shows the increase of superoxide anion levels 30 min after irradiation with 5 Gy compared with the innate production in the non-irradiated cells as shown in Fig. 1C. In Fig. 1D the elimination of superoxide anion generation (shift of the histogram to the left) in the presence of IGF-1 is obvious.

The hydrogen peroxide levels 30 min post-irradiation were 90 ± 3.48, 131 ± 5.32, 139 ± 1.77 and 158 ± 11.58 in the relative range of doses 0, 1, 2 and 5 Gy. IGF-1 presence caused a decrease in the values to 88 ± 1.25, 124 ± 1.49, 134 ± 2.48, 139 ± 13.98 after 0, 1, 2 and 5 Gy, respectively (Fig. 2A). Twenty-four hours post-irradiation with 1, 2 and 5 Gy the intracellular levels of H_2O_2 stabilized at levels similar to those of the innate generation in non-irradiated cells (Fig 2B). The presence of IGF-1 had no significant effect at the 24-h time point.

MnSOD protein expression as estimated by western blot analysis and by immunofluorescence assay

Protein expression of MnSOD was determined by immunofluorescence assay and by western blot analysis in irradiated and non-irradiated HPCs-CD34$^+$ incubated or not with IGF-1, 24 h after irradiation. As shown with western blot analysis (Fig 3A and B), irradiation of HPCs with 1, 2 and

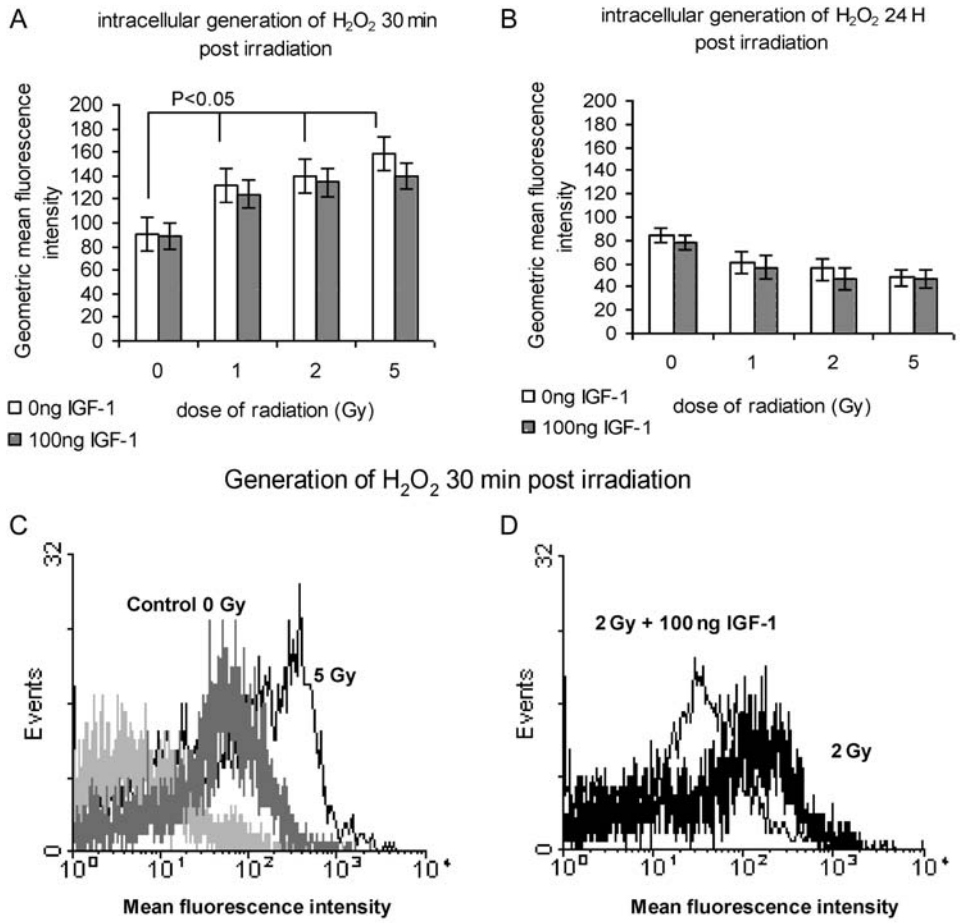

Fig. 2. Hydrogen peroxide generation in irradiated HPCs-CD34+ cells at 30 min (**A**) and at 24 h (**B**) post-irradiation with 1, 2 and 5 Gy; (C) representative histogram showing hydrogen peroxide levels in non-irradiated and cells irradiated with 5 Gy, at 30 min post-irradiation, (**D**) representative flow cytometry histogram showing the effect of IGF-1 at 2 Gy dose of radiation. The values represent mean ± SE of at least three independent experiments. In (C) the increase of the hygrogen peroxide generation is indicated by the shift of the histogram to the right; in (D) the effect of IGF-1 at a 2 Gy dose of radiation is shown by the shift of the histogram to the left.

5 Gy increased the expression of MnSOD, leading to a statistical difference among the cells irradiated with 5 Gy and the non-irradiated cells. IGF-1 presence further increased the expression of the antioxidant enzyme, leading to a statistically significant difference among irradiated and non irradiated control cells as shown in Fig. 3. The results for MnSOD expression in irradiated and non-irradiated HPCs-CD34+ with or without IGF-1 incubation were also confirmed by immunofluorescence assay (Fig. 3C).

Early and late apoptotic cells analyzed by Annexin-V and PI assay

Apoptosis of HPCs in culture as estimated by Annexin-V assay was significantly increased 6 h post-irradiation. The percentage of Annexin+ cells that represent early apoptotic cells was estimated as11.5 ± 2.01, 23.7 ± 2.17, 27 ± 1.79 and 28.5 ± 3.18 for 0, 1, 2 and 5 Gy, respectively ($P < 0.05$ versus 0 Gy; Fig. 4). At the same time point, no remarkable differences were noted at the percentage of irradiated late apoptotic cells (Annexin+ PI+) compared with non-irradiated control late apoptotic cells (7.6 ± 0.48, 12.8 ± 3.49, 13 ± 2.41 and 13.8 ± 2.93 for 0, 1, 2 and 5 Gy, respectively, $P > 0.05$ 1, 2 and 5 Gy versus non-irradiated control cells; Fig. 4).

Twenty-four hours post-irradiation, the percentage of Annexin+ cells was estimated at 13.7 ± 1.18, 15 ± 3.2, 16.7 ± 3.66 and 17 ± 2.86 for 0, 1, 2 and 5 Gy ($P > 0.05$ vs 0 Gy; Fig. 4), while the percentage of late apoptotic cells was 14.4 ± 0.79, 34 ± 6.81, 37 ± 4.17 and 42 ± 2.5 after 0, 1, 2 and 5 Gy ($P < 0.05$ for 1, 2 and 5 Gy vs 0 Gy; Fig. 4). Forty-eight hours post-irradiation the percentage of late apoptotic cells was still increasing (data not shown). It is important to point out that 24 h post-irradiation early apoptotic cells were significantly reduced compared with early

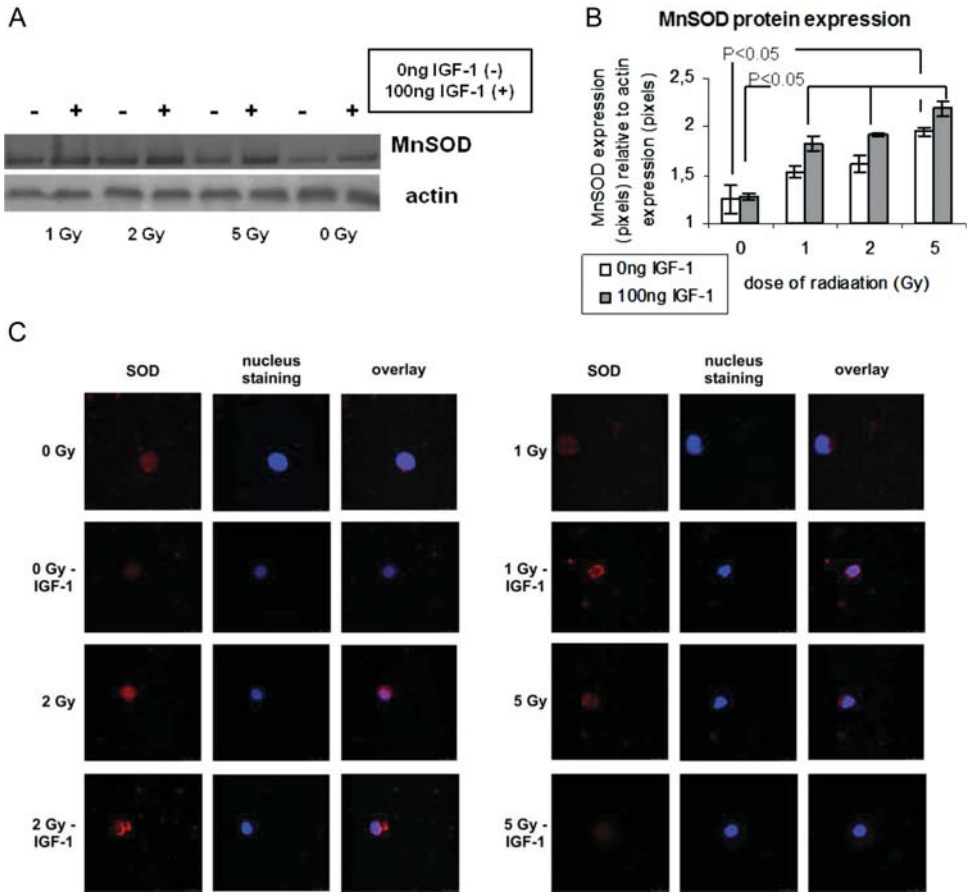

Fig. 3. MnSOD protein expression at 24 h post-irradiation relative to radiation and IGF-1 administration. (**A**) A Western blot analysis for MnSOD and actin at 24 h post-irradiation. The protein values were quantified by densitometric analysis of the corresponding bands and the ratio MnSOD protein/actin was calculated for each lane (**B**). MnSOD expression was evaluated by immunofluorescence assay. Red and blue colours show MnSOD expression and nuclear staining, respectively (**C**).

apoptotic cells at 6 h, whereas a 3-fold significant increase was noticed on late apoptotic cells at 24 h compared with late apoptotic cells at 6 h. An innate basal degree of early and late apoptosis was observed in control cells at both time points. IGF-1 presence did not affect the percentage of apoptotic cells, at the studied time points, as estimated with Annexin and PI markers (Fig. 4).

Apoptosis as manifested by DNA fragmentation

Radiation induces activation of endonucleases resulting in DNA cleavage at certain sites, giving fragments of different molecular weights. Radiation doses of 2- and 5-Gy-induced DNA fragmentation 6 h after irradiation, giving a 'smear' pattern of digested DNA [37]. The phenomenon was more intense at the 5-Gy dose (Fig. 5). At the 1-Gy dose the DNA fragmentation is not visible with this method. DNA smearing was reversed by the presence of IGF-1 at both 2 and 5 Gy (Fig. 5), instead of a laddering picture in DNA digestion we had a smear, either due to the presence of necrotic cells or due to incomplete digestion.

Apoptosis cascade molecules: BCL-2 and BAX mRNA and protein levels

We studied the effect of radiation on BCL-2 and BAX mRNA and protein levels at 4 h and 24 h, respectively, after irradiation and the effect of the presence of IGF-1. Radiation had diverse effects on the BCL-2 mRNA levels at 4 h in the presence or absence of IGF-1 (Fig. 6B). The BAX mRNA levels were up-regulated by radiation dose range, and the presence of IGF-1 decreased the BAX levels, giving statistically significant differences for the radiation doses of 1 and 2 Gy (Fig 6A). Moreover, IGF-1 administration affected the BCL-2 and BAX protein levels, 24-h post irradiation, as was evaluated by western blot analysis (Fig. 7A). It has been suggested that the BCL-2/BAX ratio may be more important than either promoter alone in determining apoptosis [38]. According to this we calculated

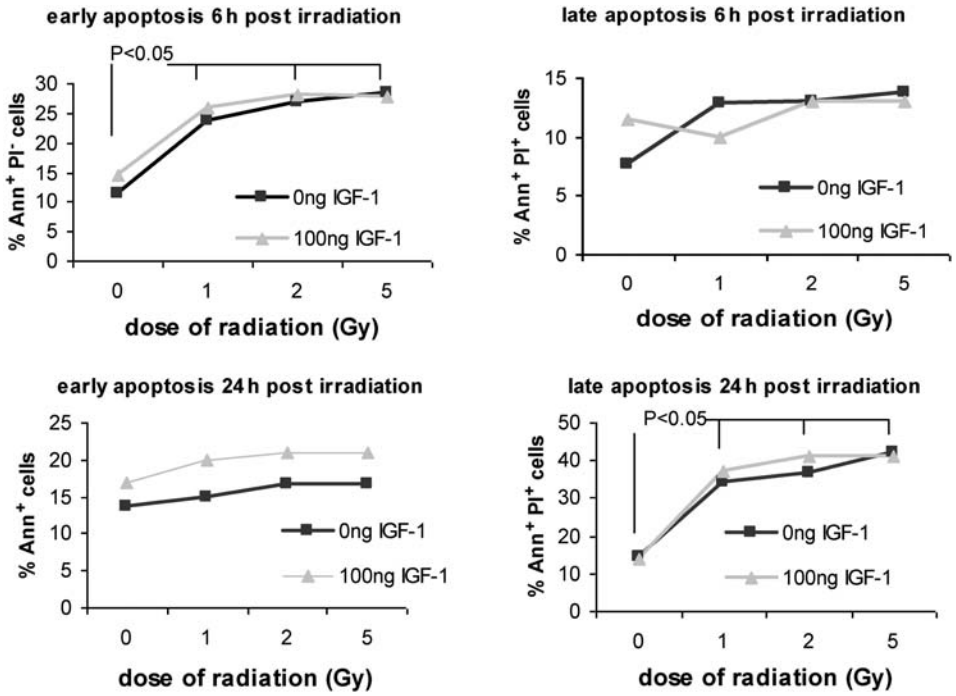

Fig. 4. The percentage of early (Ann^+ PI^-) and late (Ann^+ PI^+) apoptotic cells as estimated by Annexin-V-PI assay at 6 h and at 24 h post-irradiation. The values represent mean ± SE of at least three independent experiments.

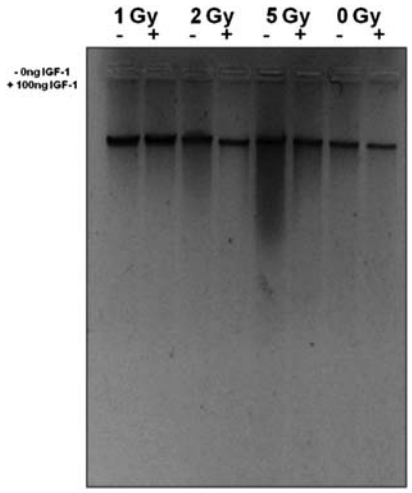

Fig. 5. Total DNA extracted from non-irradiated and irradiated HPCs at 6h post irradiation. DNA was analysed with 1.5% agarose gel electrophoresis. 1 Gy(–/+): DNA from HPCs-$CD34^+$ cells irradiated with 1 Gy with or without IGF-1; 2Gy (–/+): DNA from HPCs-CD34+ cells irradiated with 2 Gy with or without IGF-1; 5 Gy (–/+): DNA from HPCs-$CD34^+$ cells irradiated with 5 Gy with or without IGF-1; 0 Gy control cells (–/+): DNA from non-irradiated control sample HPCs-$CD34^+$ (0 Gy) with or without IGF-1.

the BCL-2/BAX ratio dividing mRNA and protein levels of BCL-2 and BAX, respectively, derived from the same experiments. Radiation caused a notable decrease of the BCL-2/BAX ratio in both mRNA and protein analysis at the doses of 1 and 2 Gy (Fig 6C and 7B). Pretreatment with IGF-1 maintained the BCL-2/BAX ratio close to the control levels (Fig 6C and 7B).

Apoptosis as estimated by caspase-9 expression

Twenty-four hours post-irradiation with therapeutic doses of 1 and 2 Gy, an up-regulation of caspase-9 levels was observed as shown by immunofluorescence colour density (Fig. 8). IGF-1 presence reduced the expression of caspase-9, indicating the anti-apoptotic role of the growth factor. This effect of IGF-1 was more evident at 2 Gy, shown as dim colour compared with the irradiated cell (Fig. 8).

Cell viability

Viability of the cells was estimated by the MTT assay, 48-h post-irradiation. Irradiation with 2 and 5 Gy suspended the viability of HPCs-$CD34^+$ as shown in Fig. 8. Pretreatment of cells with IGF-1 increased the cell viability of non-irradiated control cells and preserved it in irradiated cells (Fig. 9).

Clonogenic capacity of HPCs

The radiation doses of 1, 2 and 5 Gy significantly affected the clonogenic capacity of HPCs-$CD34^+$ cells. Irradiated HPCs-$CD34^+$ cells displayed reduced growth in semisolid short-term cultures compared with the non-irradiated controls. Colonies were small with scattered cells surrounding the aggregates. Additionally, irradiation significantly

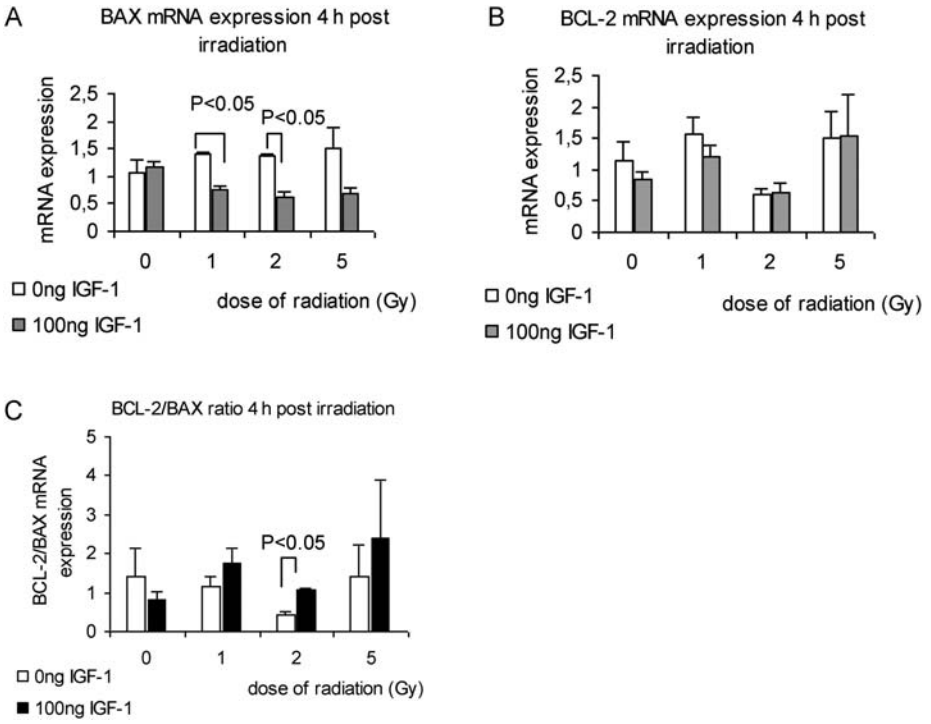

Fig. 6. The effect of radiation and IGF-1 administration on BAX mRNA expression (**A**), BCL-2 mRNA expression (**B**) and on the BCL-2/BAX ratio at 4 h post irradiation. The values represent mean ± SE of three independent experiments.

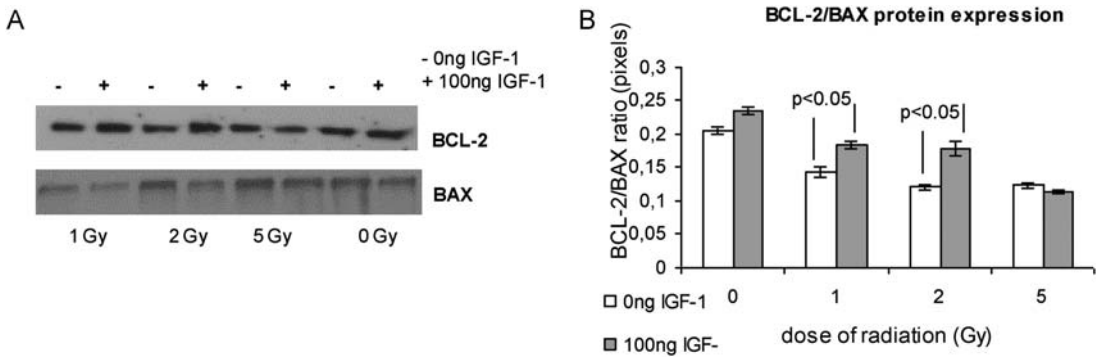

Fig. 7. BCL-2 and BAX protein expression at 24 h post-irradiation relative to radiation and IGF-1 administration. A western blot analysis is shown in (**A**). The protein amounts derived from the same experiment were quantified by densitometric analysis of the corresponding bands and the ratio BCL-2/BAX was calculated (**B**).

limited the growth of HPCs-CD34$^+$ in semi-solid media, manifested by smaller BFU-e and CFU-GM numbers of colonies compared with cultures of non-irradiated control cells ($P < 0.05$ for 1, 2 and 5 Gy versus non-irradiated control cells).

BFU-e colony numbers decreased from 103 ± 6 colonies/1000 CD34$^+$ in non-irradiated cells to 72 ± 6 colonies/1000 CD34$^+$ at 1 Gy, to 48 ± 2 colonies/1000 CD34$^+$ at 2 Gy and finally to only 2 ± 2 colonies/1000 CD34$^+$ at 5 Gy (Fig. 10B). Pretreatment of cells with IGF-1 retained the clonogenic capacity of irradiated HPCs-CD34$^+$. In particular, BFU-e colonies in IGF-1-treated cultures were 98 ± 15 after 1 Gy, 71 ± 5 after 2 Gy and 5 ± 4 after 5 Gy (Fig. 10B).

Similarly, CFU-GM colony numbers were decreased in irradiated cells in a dose-dependent manner while IGF-1 pretreatment restored the number of CFU-GM colonies. Namely, 34 ± 5, 26 ± 2 and 2 ± 1 CFU-GM colonies/1000 CD34$^+$ were counted after 1 Gy, 2 Gy and 5 Gy, respectively, while in the presence of IGF-1 these numbers were

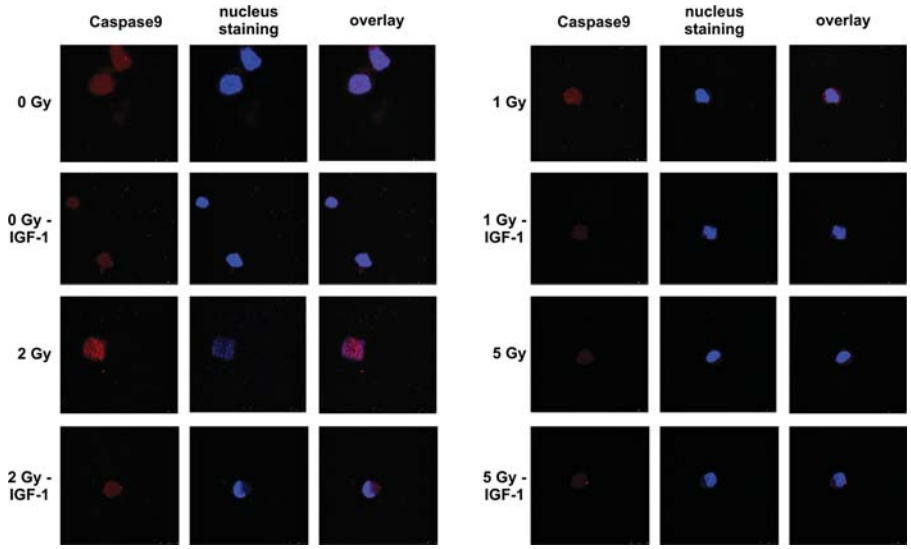

Fig. 8. Caspase-9 expression as evaluated by immunofluorescence assay. Twenty-four hours after irradiation, caspase-9 expression was evaluated on irradiated HPCs with or without IGF-1 administration as described in Methods. Red and blue colours show caspase-9 expression and nuclear staining, respectively.

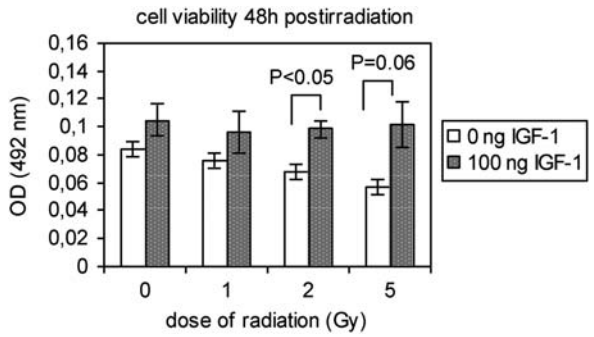

Fig. 9. The cell viability of non-irradiated and irradiated HPCs-CD34+ cells, in the presence or absence of IGF-1 supplementation at 48 h after irradiation with 1, 2 and 5 Gy. The values represent mean ± SE of at least three independent experiments.

raised to 48 ± 8, 41 ± 4 and 8 ± 6 colonies/1000 CD34+, for the same range of radiation doses ($P < 0.05$ for 2 Gy and $P = 0.07$ for 1 Gy; Fig 10A). It is important to note that in the presence of IGF-1 non-irradiated control cell colonies (BFU-e and CFU-GM) displayed a growth that was preserved even after irradiation. The results of clonogenic survival were normalized to the non-irradiated control sample, and the survival curve for CFU-GM and BFU-e colonies are presented in Fig. 10C and D, respectively.

DISCUSSION

The hematopoietic tissue is very sensitive to ionizing radiation. A dose range of 1 to 7 Gy in humans affects the hematopoietic system, resulting in the development of early and late damage in HPCs [39]. We studied a range of radiation doses from 1 to 5 Gy that represent usual therapeutic doses in fractionated radiation protocols [40, 41].

The dose of 100 ng/ml of IGF-1 is a widely used concentration as is demonstrated in previous published data [42, 43]. Moreover, the concentration of 100 ng/ml is the IGF-1 median level of normal serum as has been presented by Juul *et al.* [44]. In agreement with the above data, in our experiments, we used the dose of 100 ng/ml.

In our study, therapeutic doses of radiation rapidly increased intracellular ROS generation in HPCs-CD34+. At 30 min post-irradiation, superoxide anion levels were elevated in a dose-dependent manner, influencing the oxidative status of cells.

At the 24-h time point, the levels of superoxide anion remained high in irradiated cells compared with non-irradiated control cells. At this late time point, the increase of superoxide anion after the radiation dose of 5 Gy was probably counterbalanced because of the enhanced cellular death of irradiated cells in cultures. Moreover, at the 24-h time point, the high dose of 5 Gy was able to activate the antioxidant mechanisms of the cells that catalyse the superoxide anion to neutral products [45]. The increase in MnSOD observed in irradiated cells with 5 Gy, as evaluated by western blot analysis, confirms the above hypothesis. Pretreatment of HPCs-CD34+ with IGF-1 inhibited the intracellular superoxide anion generation at 30 min post-irradiation after doses of 2 and 5 Gy, leading to the elimination of oxidative stress in surviving cells that evade apoptosis.

Hydrogen peroxide levels remained high at 30 min post-irradiation aggravating the oxidative state of cellular

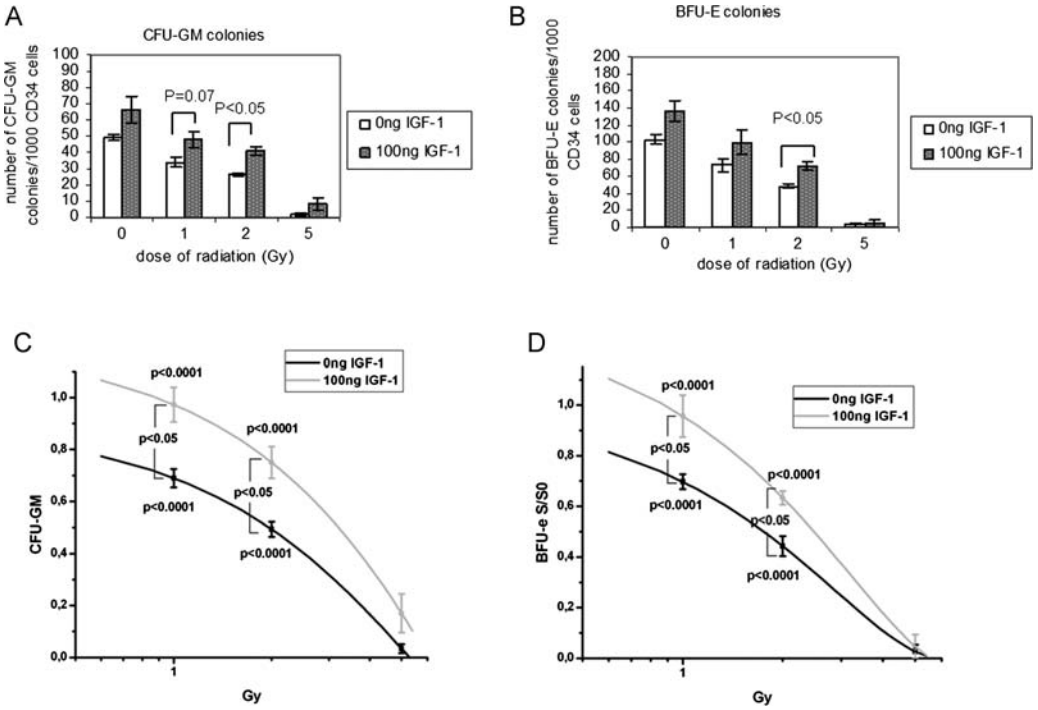

Fig. 10. Effect of radiation and IGF-1 administration on the capacity of HPCs-CD34$^+$ cells to generate CFU-GM (**A**) and BFU-e (**B**) colonies. The results of clonogenic survival were normalized to control non-irradiated sample and the survival curve for CFU-GM and BFU-e colonies are presented, respectively (**C** and **D**). The values represent mean ± SE of three independent experiments.

microenvironment, while at 24 h post-irradiation, no differences were noted among the irradiated and non-irradiated cells. At 24 h after irradiation, the intracellular production of H_2O_2 is a secondary event. Intracellular antioxidant mechanisms have probably been activated, metabolizing them to neutral products. MnSOD expression at 24 h post-irradiation supports our hypothesis about the activation of intracellular antioxidant mechanisms.

In the study by Hayashi *et al.*, the induction of superoxide anion generation in CD34$^+$ cells both at an early (4 h) and a late (16 h) time point, was shown under a high radiation dose (5 Gy), suggesting that the surviving cells may evade apoptosis and continue to proliferate, bearing increased chromosomal aberrations [10]. The same study showed that the background level of ROS in progenitor cells CD34$^+$/CD38$^+$ was higher than in CD34$^+$/CD38$^-$ immature cells, indicating that superoxide anions are generated during the continuous energy production for cell proliferation and are more pronounced in mature cells than in immature ones [10]. In our experiments, the generation of free radicals from the irradiated cell population of HPCs involves both mature and immature cells.

Following irradiation, cells appear to respond by increasing the expression of cellular antioxidant systems [46]. On the basis of these findings we assume that antioxidant mechanisms are activated around 24 h after irradiation, thus eliminating the levels of ROS by metabolizing them to neutral products. In order to confirm this hypothesis, we studied the expression of MnSOD, an antioxidant enzyme that plays a central role in protecting cells during radiation exposure. At 24 h after irradiation, an increase in the expression of MnSOD was evident, as evaluated by immunofluorescence assay and by western blot analysis corroborating the hypothesis that radiation alone activates the antioxidant mechanisms [45]. MnSOD protein expression was further enhanced by the presence of IGF-1 suggesting that IGF-1 activates the antioxidant enzyme pathways as well. Other investigators have shown the protective role of MnSOD against cytotoxicity of cells induced by IL-1. MnSOD expression in radiation-induced oxidative damage plays a central role along with other dismutases in protecting cells [47].

Several techniques widely used in apoptosis detection have been the subject of criticism. It is important to notice that apoptosis detection using Annexin-V assay may be confounded when the integrity of plasma membrane is compromised during trypsinization, Magnetic Cell Sorting (MACS) or thawing of frozen cells [48]. It is noteworthy that in our experiments, MACS was used for isolation of HPCs-CD34$^+$. The degree of apoptosis found in non-irradiated cells at the early time point of 6 h could be attributed to this. For this reason we used more than one

technique for apoptosis assessment, first, that of Annexin-V assay, which estimates changes in cellular membranes typical of early apoptosis [49], and second, DNA analysis by electrophoresis was performed in order to study DNA fragmentation. Moreover, we estimated the BCL-2 and BAX mRNA and protein levels and their ratio and caspase-9 expression, which represent mediators of the mitochondrial pathway of apoptosis known to be activated by IGF-1 [29, 16].

Pretreatment of irradiated cells with IGF-1 had no effect on apoptosis as estimated by Annexin-V assay at 6 h and 24 h post-irradiation. IGF-1 by ligation to its receptor acts on different cellular pathways and possibly bypasses the membrane network affecting the mitochondrial pathway of apoptotic cascade [28]. The unexpected results in the apoptotic assay are consistent with the observations of other investigators, who have demonstrated that phosphatidylserine exposure may be associated with circumvented cell death [50]. Hammil *et al.* showed that cells stained positive for Annexin-V are still viable and can resume growth and re-establish phospholipids' asymmetry of the membrane once the apoptotic signal is removed [50], while Span *et al.* have shown that these cells retain proliferative capacity in a single-cell, single-well assay [49].

DNA is the major target of radiation [51], and DNA fragmentation due to endonuclease activation is a hallmark of programmed cell death [52, 53]. In our experiments, this phenomenon was evident at 6 h post-irradiation and was reversed by IGF-1 administration, suggesting that a mechanism is activated by IGF-1 inhibiting the radiation-induced DNA endonuclease activation. The activity of IGF-1 on DNA degradation is in agreement with our previous work about the inhibitory effect of IGF-1 on radiation-induced apoptosis, as estimated by DNA and RNA cleavage of bone marrow mononuclear cells harvested from irradiated animals [54].

The protective effect of IGF-1 on the radiation-activated mitochondrial pathway of apoptosis was demonstrated by the changes in the mRNA and protein BCL-2, BAX and their ratio that represent potent activators of intrinsic pathway of apoptosis [17], and in the caspase-9 protein expression, a critical protein for mitochondria-dependent apoptosis [55]. The up-regulation of the anti/pro-apoptotic (BCL-2/BAX) ratio and the reduction of caspase-9 expression observed in cells pretreated with IGF-1 at doses of 1 and 2 Gy demonstrate the survival role of the factor, suggesting an inhibitory activity of IGF-1 on mitochondria-mediated programmed cell death. It is important to point out that IGF-1-induced changes in the BCL-2/BAX ratio were a result of down-regulation on BAX mRNA expression, while no effect of radiation and IGF-1 administration was noted on BCL-2 mRNA levels. In agreement with the mRNA levels, both BCL-2 and BAX protein expression were regulated by the presence of IGF-1 at 24 h post irradiation. The protective action of IGF-1 on mitochondria has also been reported by other investigators [25, 56, 26].

On the basis of the above findings in reference to the effect of IGF-1 on MnSOD, BCL-2 and BAX expression, we may conclude that overexpression of MnSOD plays a central role in the anti-apoptotic effect of the factor on HPCs by eliminating the oxidative microenvironment and by regulating the mitochondria-mediated pathway of apoptosis. The protective role of MnSOD activation and the correlation between the MnSOD and the mitochondria pathway of apoptosis have been demonstrated by other investigators [57–62].

The viability of irradiated and non-irradiated cells was also assessed. We found that cell viability as measured by the MTT assay, was suspended by irradiation and this phenomenon was reversed by IGF-1 presence. The viability assay used is based on the ability of the mitochondrial enzyme succinate dehydrogenase to metabolize MTT into formazan, a reaction that takes place only in functional intact mitochondria [63]. Taking into consideration the significant decrease in cell viability observed in irradiated cells, we may assume that these data reflect a possible dysfunction in mitochondria, where ROS are generated. IGF-1 administration restored the viability of irradiated HPCs-CD34$^+$ cells, suggesting again a possible inhibitory activity for mitochondrial ROS generation [56, 26]. Lai *et al.* have shown that doxorubicin, a drug widely used in chemotherapy, caused rapid loss of the mitochondrial electrochemical gradient and depolarization in cultured neonatal myocytes, and this was prevented by IGF-1 pre-treatment [64].

Therapeutic doses of radiation affected the clonogenic capacity of HPCs-CD34$^+$ to form BFU-e and CFU-GM colonies, in semi-solid media. IGF-1 enhanced the capacity of irradiated cells to generate BFU-e and CFU-GM colonies, supporting the role of IGF-1 as a growth and survival factor. Studies from other investigators in irradiated animals have demonstrated that IGF-1 can enhance *in vitro* growth of human hematopoietic progenitor cells and stimulate proliferation of erythroid progenitors derived from bone marrow acting as a protective factor [20, 65, 66].

It is important to point out that in most experimental procedures, statistically significant differences in ROS generation and in the protective effect of IGF-1 have been observed at a radiation dose of 2 Gy. This dose represents a common therapeutic dose per day in the field of neoplastic disease radiotherapy.

In conclusion, our data suggest that IGF-1 suppresses the oxidative microenvironment of HPCs by reducing the generation of free radicals in the intracellular environment resulting from irradiation. IGF-1 eliminates free radicals by favouring scavengering mechanisms and by regulating elements of the mitochondrial pathway of apoptosis, allowing the survival and the sustained clonogenic capacity of hematopoietic progenitor cells.

ACKNOWLEDGEMENTS

This research project is co-financed by the EU-European Social Fund (75%) and the Greek Ministry of Development-GSRT (25%) (PENED 878).

REFERENCES

1. Bowler DA, Moore SR, Mackdonald DA *et al*. Bystander-mediated genomic instability after high LET radiation in murine primary haemopoietic stem cells. *Mutat Res* 2006;**597**:50–61.
2. Wang Y, Liu L, Pazhanisamy SK *et al*. Total body irradiation causes residual bone marrow injury by induction of persistent oxidative stress in murine hematopoietic stem cells. *Free Radic Biol Med* 2010;**48**:348–356.
3. Valko M, Leibfritz D, Moncol J *et al*. Free radicals and antioxidants in normal physiological functions and human disease. *Int J Biochem Cell Biol* 2007;**39**:44–84.
4. Tominaga H, Kodama S, Matsuda N *et al*. Involvement of reactive oxygen species (ROS) in the induction of genetic instability by radiation. *J Radiat Res (Tokyo)* 2004;**45**:181–8.
5. Zamzami N, Marchetti P, Castedo M *et al*. Sequential reduction of mitochondrial transmembrane potential and generation of reactive oxygen species in early programmed cell death. *J Exp Med* 1995;**182**:367–77.
6. Fachin AL, Mello SS, Sandrin-Garcia P *et al*. Gene expression profiles in radiation workers occupationally exposed to ionizing radiation. *J Radiat Res (Tokyo)* 2009;**50**:61–71.
7. Harper K, Lorimore SA, Wright EG. Delayed appearance of radiation-induced mutations at the Hprt locus in murine hemopoietic cells. *Exp Hematol* 1997;**25**:263–9.
8. El-Osta A. The rise and fall of genomic methylation in cancer. *Leukemia* 2004;**18**:233–7.
9. Huang L, Snyder AR, Morgan WF. Radiation-induced genomic instability and its implications for radiation carcinogenesis. *Oncogene* 2003;**22**:5848–54.
10. Hayashi T, Hayashi I, Shinohara T *et al*. Radiation-induced apoptosis of stem/progenitor cells in human umbilical cord blood is associated with alterations in reactive oxygen and intracellular pH. *Mutat Res* 2004;**556**:83–91.
11. Narayanan PK, Goodwin EH, Lehnert BE. Alpha particles initiate biological production of superoxide anions and hydrogen peroxide in human cells. *Cancer Res* 1997;**57**:3963–71.
12. Morgan WF. Non-targeted and delayed effects of exposure to ionizing radiation: II. Radiation-induced genomic instability and bystander effects in vivo, clastogenic factors and transgenerational effects. *Radiat Res* 2003;**159**:581–96.
13. Limoli CL, Giedzinski E, Morgan WF *et al*. Persistent oxidative stress in chromosomally unstable cells. *Cancer Res* 2003;**63**:3107–11.
14. Pajovic SB, Joksic G, Kasapovic J *et al*. Role of antioxidant enzymes in radiosensitivity of human blood cells. *J Environ Pathol Toxicol Oncol* 2000;**19**:325–31.
15. Simon HU, Haj-Yehia A, Levi-Schaffer F. Role of reactive oxygen species (ROS) in apoptosis induction. *Apoptosis* 2000;**5**:415–18.
16. Korsmeyer SJ. Regulators of cell death. *Trends Genet* 1995;**11**:101–5.
17. Korsmeyer SJ, Shutter JR, Veis DJ *et al*. Bcl-2/Bax: a rheostat that regulates an anti-oxidant pathway and cell death. *Semin Cancer Biol* 1993;**4**:327–32.
18. Oltvai ZN, Milliman CL, Korsmeyer SJ. Bcl-2 heterodimerizes in vivo with a conserved homolog, Bax, that accelerates programmed cell death. *Cell* 1993;**74**:609–19.
19. Salvesen GS, Dixit VM. Caspases: intracellular signaling by proteolysis. *Cell* 1997;**91**:443–6.
20. Carlo-Stella C, Di Nicola M, Milani R *et al*. Age- and irradiation-associated loss of bone marrow hematopoietic function in mice is reversed by recombinant human growth hormone. *Exp Hematol* 2004;**32**:171–8.
21. Drouet M, Mathieu J, Grenier N *et al*. Single administration of stem cell factor, FLT-3 ligand, megakaryocyte growth and development factor, and interleukin-3 in combination soon after irradiation prevents nonhuman primates from myelosuppression: long-term follow-up of hematopoiesis. *Blood* 2004;**103**:878–85.
22. Majka M, Janowska-Wieczorek A, Ratajczak J *et al*. Numerous growth factors, cytokines, and chemokines are secreted by human CD34(+) cells, myeloblasts, erythroblasts, and megakaryoblasts and regulate normal hematopoiesis in an autocrine/paracrine manner. *Blood* 2001;**97**:3075–85.
23. Peruzzi F, Prisco M, Dews M *et al*. Multiple signaling pathways of the insulin-like growth factor 1 receptor in protection from apoptosis. *Mol Cell Biol* 1999;**19**:7203–15.
24. Abboud SL, Bethel CR, Aron DC. Secretion of insulinlike growth factor I and insulinlike growth factor-binding proteins by murine bone marrow stromal cells. *J Clin Invest* 1991;**88**:470–5.
25. Pang Y, Zheng B, Fan LW *et al*. IGF-1 protects oligodendrocyte progenitors against TNFalpha-induced damage by activation of PI3K/Akt and interruption of the mitochondrial apoptotic pathway. *Glia* 2007;**55**:1099–107.
26. Pi Y, Goldenthal MJ, Marin-Garcia J. Mitochondrial involvement in IGF-1 induced protection of cardiomyocytes against hypoxia/reoxygenation injury. *Mol Cell Biochem* 2007;**301**:181–9.
27. Kulik G, Klippel A, Weber MJ. Antiapoptotic signalling by the insulin-like growth factor I receptor, phosphatidylinositol 3-kinase, and Akt. *Mol Cell Biol* 1997;**17**:1595–606.
28. Kurmasheva RT, Houghton PJ. IGF-I mediated survival pathways in normal and malignant cells. *Biochim Biophys Acta* 2006;**1766**:1–22.
29. Chitnis MM, Yuen JS, Protheroe AS *et al*. The type 1 insulin-like growth factor receptor pathway. *Clin Cancer Res* 2008;**14**:6364–70.
30. Ivanovic Z Hematopoietic stem cells in research and clinical applications: the 'CD34 issue'. *World J Stem Cells* 2010;**2**:18–23.
31. Mylonas PG, Matsouka PT, Papandoniou EV *et al*. Growth hormone and insulin-like growth factor I protect intestinal cells from radiation induced apoptosis. *Mol Cell Endocrinol* 2000;**160**:115–22.
32. Sarkar M, Varshney R, Chopra M *et al*. Flow-cytometric analysis of reactive oxygen species in peripheral blood mononuclear cells of patients with thyroid dysfunction. *Cytometry B Clin Cytom* 2006;**70**:20–3.

33. Grivas PD, Antonacopoulou A, Tzelepi V *et al*. HER-3 in colorectal tumourigenesis: from mRNA levels through protein status to clinicopathologic relationships. *Eur J Cancer* 2007;**43**:2602–11.
34. Rozen S, Skaletsky H. Primer3 on the WWW for general users and for biologist programmers. *Methods Mol Biol* 2000;**132**:365–86.
35. Bagley J, Rosenzweig M, Marks DF *et al*. Extended culture of multipotent hematopoietic progenitors without cytokine augmentation in a novel three-dimensional device. *Exp Hematol* 1999;**27**:496–504.
36. Michalopoulou S, Micheva I, Kouraklis-Symeonidis A *et al*. Impaired clonogenic growth of myelodysplastic bone marrow progenitors *in vitro* is irrelevant to their apoptotic state. *Leuk Res* 2004;**28**:805–12.
37. Sasano N, Enomoto A, Hosoi Y *et al*. Free radical scavenger edaravone suppresses x-ray-induced apoptosis through pp53 inhibition in MOLT-4 cells. *J Radiat Res (Tokyo)* 2007;**48**:495–503.
38. Del Poeta G, Venditti A, Del Principe MI *et al*. Amount of spontaneous apoptosis detected by Bax/Bcl-2 ratio predicts outcome in acute myeloid leukemia (AML). *Blood* 2003;**101**:2125–31.
39. Mauch P, Constine L, Greenberger J *et al*. Hematopoietic stem cell compartment: acute and late effects of radiation therapy and chemotherapy. *Int J Radiat Oncol Biol Phys* 1995;**31**:1319–39.
40. Campbell BA, Voss N, Woods R *et al*. Long-term outcomes for patients with limited stage follicular lymphoma: involved regional radiotherapy versus involved node radiotherapy. *Cancer* 2010;**116**:3797–806.
41. Dimopoulos MA, Goldstein J, Fuller L *et al*. Curability of solitary bone plasmacytoma. *J Clin Oncol* 1992;**10**:587–90.
42. Barres BA, Hart IK, Coles HS *et al*. Cell death and control of cell survival in the oligodendrocyte lineage. *Cell* 1992;**70**:31–46.
43. Frostad S, Bjerknes R, Abrahamsen JF *et al*. Insulin-like growth factor-1 (IGF-1) has a costimulatory effect on proliferation of committed progenitors derived from human umbilical cord CD34+ cells. *Stem Cells* 1998;**16**:334–42.
44. Juul A, Bang P, Hertel NT *et al*. Serum insulin-like growth factor-I in 1030 healthy children, adolescents, and adults: relation to age, sex, stage of puberty, testicular size, and body mass index. *J Clin Endocrinol Metab* 1994;**78**:744–52.
45. Summers RW, Maves BV, Reeves RD *et al*. Irradiation increases superoxide dismutase in rat intestinal smooth muscle. *Free Radic Biol Med* 1989;**6**:261–70.
46. Spitz DR, Azzam EI, Li JJ *et al*. Metabolic oxidation/reduction reactions and cellular responses to ionizing radiation: a unifying concept in stress response biology. *Cancer Metastasis Rev* 2004;**23**:311–22.
47. Sun J, Chen Y, Li M *et al*. Role of antioxidant enzymes on ionizing radiation resistance. *Free Radic Biol Med* 1998;**24**:586–93.
48. Darzynkiewicz Z, Bedner E, Smolewski P. Flow cytometry in analysis of cell cycle and apoptosis. *Semin Hematol* 2001;**38**:179–93.
49. Span LF, Pennings AH, Vierwinden G *et al*. The dynamic process of apoptosis analyzed by flow cytometry using Annexin-V/propidium iodide and a modified in situ end labeling technique. *Cytometry* 2002;**47**:24–31.
50. Hammill AK, Uhr JW, Scheuermann RH. Annexin V staining due to loss of membrane asymmetry can be reversible and precede commitment to apoptotic death. *Exp Cell Res* 1999;**251**:16–21.
51. Isabelle V, Prevost C, Spotheim-Maurizot M *et al*. Radiation-induced damages in single- and double-stranded DNA. *Int J Radiat Biol* 1995;**67**:169–76.
52. Montague JW, Cidlowski JA. Cellular catabolism in apoptosis: DNA degradation and endonuclease activation. *Experientia* 1996;**52**:957–62.
53. Nagata S. Apoptotic DNA fragmentation. *Exp Cell Res* 2000;**256**:12–18.
54. Matsouka P, Mylonas P, Papandoniou E *et al*. Abdominal radiation initiates apoptotic mechanism in rat femur bone marrow cells in vivo that is reversed by IGF-1 administration. *J Radiat Res (Tokyo)* 2008;**49**:41–7.
55. Green DR, Kroemer G. The pathophysiology of mitochondrial cell death. *Science* 2004;**305**:626–9.
56. Perez R, Garcia-Fernandez M, Diaz-Sanchez M *et al*. Mitochondrial protection by low doses of insulin-like growth factor-I in experimental cirrhosis. *World J Gastroenterol* 2008;**14**:2731–9.
57. Epperly MW, Bernarding M, Gretton J *et al*. Overexpression of the transgene for manganese superoxide dismutase (MnSOD) in 32D cl 3 cells prevents apoptosis induction by TNF-alpha, IL-3 withdrawal, and ionizing radiation. *Exp Hematol* 2003;**31**:465–74.
58. Epperly MW, Epperly LD, Niu Y *et al*. Overexpression of the MnSOD transgene product protects cryopreserved bone marrow hematopoietic progenitor cells from ionizing radiation. *Radiat Res* 2007;**168**:560–6.
59. Holley AK, Dhar SK, Xu Y *et al*. Manganese superoxide dismutase: beyond life and death. *Amino Acids* 2010;**42**:139–58.
60. Holley AK, Xu Y, St Clair DK *et al*. RelB regulates manganese superoxide dismutase gene and resistance to ionizing radiation of prostate cancer cells. *Ann N Y Acad Sci* 2010;**1201**:129–36.
61. Li WJ, Shin MK, Oh SJ. Time dependent bladder apoptosis induced by acute bladder outlet obstruction and subsequent emptying is associated with decreased MnSOD expression and Bcl-2/Bax ratio. *J Korean Med Sci* 2010;**25**:1652–6.
62. Stohr O, Hahn J, Moll L *et al*. Insulin receptor substrate-1 and -2 mediate resistance to glucose-induced caspase-3 activation in human neuroblastoma cells. *Biochim Biophys Acta* 2011;**1812**:573–80.
63. Dreiem A, Gertz CC, Seegal RF. The effects of methylmercury on mitochondrial function and reactive oxygen species formation in rat striatal synaptosomes are age-dependent. *Toxicol Sci* 2005;**87**:156–62.
64. Lai HC, Liu TJ, Ting CT *et al*. Insulin-like growth factor-1 prevents loss of electrochemical gradient in cardiac muscle mitochondria via activation of PI 3 kinase/Akt pathway. *Mol Cell Endocrinol* 2003;**205**:99–106.
65. Goff JP, Shields DS, Boggs SS *et al*. Effects of recombinant cytokines on colony formation by irradiated human cord blood CD34+ hematopoietic progenitor cells. *Radiat Res* 1997;**147**:61–9.
66. Miyagawa S, Kobayashi M, Konishi N *et al*. Insulin and insulin-like growth factor I support the proliferation of erythroid progenitor cells in bone marrow through the sharing of receptors. *Br J Haematol* 2000;**109**:555–62.